JPn Neuroscience

The Journal of Physiology

J Physiol 591.1 (2013) pp 339–352

Multiple pathways carry signals from short-wavelength-sensitive ('blue') cones to the middle temporal area of the macaque

Jaikishan Jayakumar[1], Sujata Roy[1], Bogdan Dreher[2], Paul R. Martin[3] and Trichur R. Vidyasagar[1]

[1] *Department of Optometry and Vision Sciences, The University of Melbourne, Australia*
[2] *Discipline of Anatomy & Histology, School of Medical Sciences & Bosch Institute, University of Sydney, Australia*
[3] *ARC Centre of Excellence in Vision Science, Save Sight Institute and Discipline of Physiology, University of Sydney, Australia*

Key points

- The middle temporal area (area MT) of the macaque visual cortex receives visual signals from all three cone types, including short-wavelength cones (S-cones).
- Signals from the short-wavelength cones reach area MT both via the relay(s) in the primary visual cortex (V1) as well as a pathway bypassing V1.
- The S-cone signals to area MT that bypass V1 do not reach area MT significantly earlier than those that relay through V1.
- The S-cone signals that bypass V1 are most likely conveyed to area MT by direct projections from the koniocellular regions of the dorsal lateral geniculate nucleus.
- Our results are consistent with the putative neuronal mechanism of the phenomenon of 'blindsight'.

Abstract We recorded spike activity of single neurones in the middle temporal visual cortical area (MT or V5) of anaesthetised macaque monkeys. We used flashing, stationary spatially circumscribed, cone-isolating and luminance-modulated stimuli of uniform fields to assess the effects of signals originating from the long-, medium- or short- (S) wavelength-sensitive cone classes. Nearly half (41/86) of the tested MT neurones responded reliably to S-cone-isolating stimuli. Response amplitude in the majority of the neurones tested further (19/28) was significantly reduced, though not always completely abolished, during reversible inactivation of visuotopically corresponding regions of the ipsilateral primary visual cortex (striate cortex, area V1). Thus, the present data indicate that signals originating in S-cones reach area MT, either via V1 or via a pathway that does not go through area V1. We did not find a significant difference between the mean latencies of spike responses of MT neurones to signals that bypass V1 and those that do not; the considerable overlap we observed precludes the use of spike-response latency as a criterion to define the routes through which the signals reach MT.

(Resubmitted 18 July 2012; accepted after revision 10 October 2012; first published online 15 October 2012)
Corresponding author T. R. Vidyasagar: Department of Optometry and Vision Sciences, The University of Melbourne, Parkville VIC 3010, Australia. Email: trv@unimelb.edu.au

Abbreviations DSI, direction selectivity index; LGN, dorsal lateral geniculate nucleus; MST, medial superior visual cortical temporal area; MT, middle temporal visual cortical area; PSTH, peristimulus time histogram; RF, receptive field; S-cones, short-wavelength-sensitive cones; V1, primary visual cortex.

DOI: 10.1113/jphysiol.2012.241117

Introduction

Since the early reports of functional specialisation within the visual areas of the primate cerebral neocortex (Zeki, 1978), studies of the middle temporal area (MT or area V5) of macaque monkeys concentrated on analysis of processing of information about motion rather than chromaticity (e.g. DeYoe & Van Essen, 1988; Livingstone & Hubel, 1988). However, more recently, substantial evidence has accumulated indicating that the 'motion-analysing' MT neurones do respond to iso-luminant chromatic stimuli (Saito *et al.* 1989; Dobkins & Albright, 1994; Gegenfurtner *et al.* 1994; Gegenfurtner & Hawken, 1996; Seidemann *et al.* 1999; Barberini *et al.* 2005; Riecansky *et al.* 2005).

Area MT is normally considered to receive its principal visual inputs from neurones in the magnocellular layers of the dorsal lateral geniculate nucleus (LGN) through projections relayed via neurones in layer 4B of area V1 (striate cortex, primary visual cortex), and via cells in the so-called thick cytochrome oxidase-rich stripes in area V2 (Maunsell & van Essen, 1983; Livingstone & Hubel, 1988). In addition, area MT receives a direct projection from the koniocellular layers of the LGN (Sincich *et al.* 2004) and also some inputs from the parvocellular layers of the LGN (Maunsell *et al.* 1990), most likely relayed through layer 6 cells of V1 (Nassi *et al.* 2006). Studies using functional magnetic resonance imaging (Wandell *et al.* 1999) or visually evoked potentials (Morand *et al.* 2000) reported that human area MT receives inputs from the short-wavelength-sensitive cones (S-cones). The pathway(s) through which the putative S-cone signals reach area MT is, however, not known. Furthermore, whether S-cones provide a functional input to area MT of macaque monkeys is itself in debate. While some studies reported that macaque's MT neurones respond to S-cone signals (Seidemann *et al.* 1999; Barberini *et al.* 2005; Riecansky *et al.* 2005), others have questioned the existence of an S-cone input to MT (Gegenfurtner *et al.* 1994).

In macaque monkeys, area MT neurones are reported to respond to visual stimuli even after an ablation (Rodman *et al.* 1989) or reversible inactivation (Girard *et al.* 1992) of ipsilateral area V1. Any direct projection to area MT that bypasses area V1 is of both heuristic and clinical interest in the context of the phenomenon of 'blindsight' experienced by patients with damage to V1 (e.g. Weiskrantz *et al.* 1974; Cowey, 2004; Vakalopoulos, 2005),

In the present study we have examined: (1) if single neurones in macaque area MT respond reliably to S-cone-isolating stimuli; (2) whether signals originating from S-cones arrive in area MT via area V1 or bypass V1; and (3) whether the direct subcortical signals to MT arrive significantly earlier than those relayed via V1. We performed the reversible inactivation of topographically corresponding part of ipsilateral area V1 either by cooling (using a Peltier device) or by microiontophoresis of the inhibitory transmitter GABA. Preliminary results were published in the form of an abstract (Jayakumar *et al.* 2009).

Methods

Surgical preparation

Experiments were conducted on five adult male pigtailed macaques (*Macaca nemestrina*, weighing between 3.3 and 4.5 kg). All procedures were approved by the Animal Ethics Committee of the University of Melbourne, and conformed to NIH guidelines and the Australian National Health and Medical Research Council code of practice for the care and use of animals for scientific purposes. After initial induction of anaesthesia with ketamine (15 mg kg^{-1}; I.M.; Ketamil, Parnell Laboratories, Australia) and xylazine (2 mg kg^{-1}; I.M.; Ilium Xylazil-20, Troy Laboratories, Australia), cephalic veins in both forelimbs were catheterised and the trachea was cannulated. A thermistor was surgically inserted behind the scapula for monitoring temperature and providing feedback to a servo-controlled heating blanket that maintained the body temperature at ∼36°C. Skeletal muscle paralysis was induced with a dose of vecuronium (Norcuron, Organon Australia Pty Ltd; 0.7 mg kg^{-1}, I.V.). Anaesthesia and muscle paralysis were maintained with sufentanil (Sufenta forte, Janssen-Cilag Australia; 3–6 μg kg^{-1} h^{-1}) and vecuronium (0.2 mg kg^{-1} h^{-1}) respectively. These drugs and dexamethasone (0.1 mg h^{-1}; Mayne Pharma (Pty) Ltd, Australia) in 5% glucose were administered through one of the venous catheters. The second catheter was used for a slow infusion of 5% glucose in normal saline to maintain a total intake of fluid of approximately 100–200 ml day^{-1}. All pressure points were anaesthetised locally using xylocaine ointment (2% lignocaine hydrochloride; Astra-Zeneca, Australia). End tidal carbon dioxide was maintained between 3.6% and 3.8%. ECG and EEG were recorded to assess the depth of anaesthesia, and the dosage of sufentanil was adjusted to maintain surgical anaesthesia.

A wide craniotomy (Horsley–Clark coordinates posterior 0–28 mm, lateral 1–22 mm) was performed to expose the dura over the superior-temporal sulcus and much of the dorsal aspect of the occipital lobe. Small durotomies were made to enable electrode insertions into MT. The penetrations aimed at area MT were usually in the parasagittal plane about 15 mm lateral to the midline, and angled either vertically or up to 30 deg anteriorly from the vertical (see Lagae *et al.* 1994). Because there is considerable variation in the visuotopy and the stereotaxic co-ordinates of MT from one macaque to the other, and it was also essential to record from cells whose receptive fields (RFs) overlapped with the RFs of cells at the site of

inactivation in V1, a number of penetrations were made until the appropriate region of area MT was reached. Epoxy-coated tungsten microelectrodes (4–10 Mohms; Frederick Haer Co., Bowdoinham, ME, USA) were used for recording extracellular potentials. The pupils were dilated using atropine (Atropt 1%; Sigma Pharmaceuticals Pty Ltd, Australia), and gas-permeable contact lenses were used to protect the cornea. Trial lenses of appropriate dioptric powers were used to focus the eyes onto a monitor placed 114 cm from the pupil plane. A fundus camera with a rear projector attachment was used to record the positions of the foveas, optic discs and their surrounding vasculature at regular intervals.

Visual stimuli

After initial hand plotting of the minimum discharge fields (e.g. Barlow *et al.* 1967), drifting achromatic (luminance-modulated) gratings were used to centre the RFs on to a Reference Calibrator Plus (BARCO, Kortrijk, Belgium) monitor with a frame rate of 75 Hz located 114 cms in front of the animal. Achromatic (luminance-modulated) gratings were used to obtain the optimum characteristics such as orientation tuning, spatial frequency tuning and temporal frequency tuning for MT neurones. Visual stimuli were generated and presented on a Macintosh G4 computer using EXPO (Core Vision, Centre for Neural Science, University of New York, USA) using Open GL commands. The cone-isolating stimuli were based on the Lamb nomograms (Lamb, 1995) of peak wavelengths at 560 nm, 530 nm and 430 nm. Lens absorbance was corrected using published values for human lens (Wyszecki & Stiles, 1982). The effect of receptor self-screening was estimated assuming axial absorbance of 1.5% and outer segment length 20 μm. No correction for macular pigment was made. Cone-isolating stimuli were calculated by convolution of the predicted corneal cone fundamentals with the monitor's [R, G, B] phosphor spectral distribution. Flashing, spatially uniform stimuli (0.5–4 Hz square wave modulation within apertures ranging from 2 to 6 deg), with S-cone contrast reversal and achromatic luminance contrast reversal, were used to stimulate area MT neurones. The contrast-reversing stimuli were between CIE coordinates [x, y, Y: 0.281, 0.243, 36.1] and [0.377, 0.503, 36.7] for the S-cone isolating stimuli, and [0.311, 0.324, 67.1] and [0.311, 0.324, 3.61] for luminance-modulated stimuli. The stimuli were presented in a random fashion and interleaved with a blank screen held at a mean luminance of 36.4 cd m^{-2}. The spectral power distribution of the monitor guns and the colour coordinates of the cone-isolating stimuli were verified using a PR-650 Photometer (Photo Research, Palo Alto, California, USA). Contrast sensitivity curves reported in this paper were obtained for nine different contrast levels (3%, 5%, 7%, 11%, 18%, 27%, 42%, 65% and 100%) for both the luminance stimuli and S-cone stimuli, with the exception that the highest contrast achievable for S-cone modulation was 80%. The mean luminance of the flashing stimuli and the moving grating stimuli were the same for both the S-cone-isolating and luminance-modulating stimuli, and same as the blank screen (within measurement error).

Electrophysiological recordings

Neuronal activity in area MT was recorded using an AM systems differential amplifier (AM systems Inc, Carlsborg, WA, USA). These signals were bandpass filtered (300–5000 Hz) and recorded through the computer audio input (sampling rate 22,000 Hz). Individual spikes were identified and clustered using principal component analysis. Peristimulus time histograms (PSTHs) of the spiking responses were generated for each stimulus and were used for further analysis.

Neurones with visual input were classified as those that had firing rates in response to visual stimuli significantly greater (>95% confidence) than the maintained discharge for a blank screen of same average luminance. Cells with S-cone input were identified as those that had peak firing rates in response to S-cone-isolating stimulus significantly greater than the maintained discharge for a blank screen. Peak firing rates were calculated from PSTHs over a 20 ms bin with no smoothing and without removal of spontaneous firing rate. We also calculated a S-cone sensitivity index as the peak response to S-cone modulation (with 80% S-cone contrast) divided by the peak response to achromatic modulation (with 100% luminance contrast). A cell with a weak S-cone input would thus have a low S-cone sensitivity index compared with a cell with a strong S-cone input. When measuring contrast sensitivity function using moving gratings, we performed a fast Fourier transform of the response and used the zero harmonic component (mean discharge frequency) for the analysis. The stimulus set did include medium (M)-cone- and long (L)-cone-isolating stimuli, but in this study we will be presenting only the results pertaining to S-cone and luminance (L + M)-modulating stimuli.

The latencies of spike responses of area MT neurones were calculated using the criteria previously established by Maunsell & Gibson (1992). The PSTHs were plotted without smoothing using 1 ms bins. The latency value was read off the first bin in which the number of spikes was at least three SDs above the background activity, followed by two consecutive bins with number of spikes at least two SDs above background. The average of at least 500 bins (of 1 ms bin width) of spike activity to a blank screen was defined as the background activity.

Reversible inactivation of V1 with cooling

A custom-built thermoelectric Peltier device with a silver plate that mimicked the curvature of the dorsal aspect of the macaque's V1 was placed over V1 to achieve reversible cooling. The Peltier device was based on a design described elsewhere (Girard & Bullier, 1989). The temperature of the cortex below the device was measured using a thermocouple placed within a glass micropipette inserted through an aperture in the silver plate. Reversal of temperature gradient was achieved by changing the polarity of the current used. The desired and stable temperature of the device was usually achieved within 10 min. The temperature at 1 mm below surface after 9 min of cooling when the surface was cooled to 2.8°C was 10°C. This result was similar to those obtained by Girard & Bullier (1989), and is sufficient to cause complete suppression of spike activity in V1 (Volgushev *et al.* 2000). We avoided keeping the cortex cooled for more than 30 min so as not to irreversibly damage it. Despite this precaution, in a few cases, the magnitude of responses of the MT cell did not recover fully before the recording was lost.

In all animals, we placed the anterior border of the Peltier probe close to the lunate sulcus. Because the V1/V2 border representing the vertical meridian runs just posterior to the lunate sulcus (Gattass *et al.* 1981), our method gives consistency of placement across all the animals, at least along the vertical meridian. To enable the Peltier to cover as much of the visual field on the dorsal striate surface as possible, the medial border of the Peltier probe was positioned not far from the midline (2–2.5 mm) and so the lateral edge of the Peltier probe was positioned as far away as possible from the horizontal meridian representation. We thus avoided the very centre of the fovea (much of the foveola), which has a much higher cortical magnification factor. To be certain that parts of area V1 excited by the visual stimulus were indeed inactivated sufficiently, the visual stimulus was largely confined to within a square of approximately 6×6 deg inferolateral from the fovea, but mostly or entirely within the RF of the MT cell. Our aim was to ensure that the signals that reached MT via V1 were relayed through the part of V1 that was accessible to our cooling probe; this meant that the stimuli were not necessarily centred on the RF of the MT neurone that we recorded from. This approach was similar to that used by Girard & Bullier (1989). See later (Results, and Figs 5 and 6) for controls and data analysis that ensured the adequacy of this method for our study.

GABA inactivation of V1

In one macaque, we studied the responses of area MT neurones before and during iontophoretic application of the inhibitory neurotransmitter, GABA, within the topographically corresponding location in V1. A glass micropipette assembly made of four individual glass micropipettes each with an inner tip diameter of approximately 5 μm was glued to a tungsten-in-glass microelectrode (4 MΩ) using an ultraviolet curable glue (NOA 801, Norland Products, Cranbury, NJ, USA). The tips of the micropipettes were separated by 250 μm from the tip of the tungsten electrode. This distance was calculated on the basis of the estimate (cf. Hupé *et al.* 1999) that each GABA micropipette would inactivate 300 μm of cortex around it. Thus, the separation of the four micropipettes would result in inactivation of a visual field area ∼2 deg in diameter at an eccentricity of 4 deg. This value was calculated from the published values of the relationship between cortical magnification factor, RF size, RF scatter and eccentricity (Dow *et al.* 1981). The micropipettes were filled with 0.5 M (pH 3–3.5) GABA solution (Sigma Pharmaceuticals Pty Ltd). The filled micropipette assembly had a retaining current of −5 to −10 nA. To achieve complete suppression of V1 spike responses, GABA was iontophoretically ejected using current pulses that varied between +100 nA and +200 nA. The visuotopic extent of the part of area V1 inactivated by GABA usually did not cover the entire region corresponding topographically to the RF of MT neurones recorded from. Therefore, we confined the visual stimulus to the part of the visual field that was represented in the inactivated part of area V1 as determined by the location of RFs of cells recorded by the microelectrode positioned in the middle of the V1 micropipette assembly.

Histology

Electrolytic lesions were made at a number of locations in each penetration. At the end of the experiment, after intravenous administration of heparin (1000 IU) and a lethal dose (120 mg kg^{-1}) of sodium pentobarbitone (Nembutal), the monkeys were transcardially perfused with 4% paraformaldehyde and the brain processed for histology. Alternate 50 μm sections were stained with Cresyl violet for Nissl substance and a silver stain for myelin. Reconstructions of electrode tracks using lesion sites in Cresyl violet sections and inspection of the myelin stain sections to identify area MT were used as final arbiters of the recording sites.

Results

We recorded single-unit activities of 86 area MT neurones. In most cases, at the beginning of the penetration along the superior temporal sulcus, the electrode moved into the medial superior temporal area (MST area). Area MST, like area MT, contains neurones that are characterised by their vigorous direction-selective spike responses to

rapidly moving visual stimuli. Consistent with earlier reports (e.g. Komatsu & Wurtz, 1988; Lagae *et al.* 1994), as the electrode moved out of area MST into putative area MT, the RFs of newly encountered neurones were smaller. Quantitative data on direction selectivity using drifting grating stimuli were collected in 47 of the area MT cells. The mean direction selectivity index (DSI) was calculated as follows:

$$\mathrm{DSI} = 1 - (R_{\mathrm{nonpref}}/R_{\mathrm{pref}}),$$

where R_{pref} is the response in the most preferred direction and R_{nonpref} is the response in the opposite direction (Albright, 1984). R_{pref} is the peak response of the MT neurone (firing rate averaged over 20 ms bins) in response to a grating drifting in the preferred direction of the neuron. R_{nonpref} is the peak response of the neurone to a grating drifting in the direction opposite to the preferred direction. With moving grating stimuli, most cells exhibited a high degree of direction selectivity with a mean DSI of 0.80 (SD $\pm$ 0.25) for our sample. Almost half of our sample of area MT neurones (41/86; 47.5%) responded reliably not only to moving and stationary luminance-modulated stimuli (e.g. Fig. 1*A*, upper PSTH), but also to flashing stationary S-cone-isolating stimuli (e.g. Fig. 1*A*, lower PSTH). The remaining MT cells (45/86; 52.5%) showed robust responses to luminance modulation (e.g. Fig. 2*B*, upper PSTH), but no significant responses to S-cone-isolating stimuli (e.g. Fig. 1*B*, lower PSTH). This result implies that S-cone signals reach about half the cells in area MT. There is, however, one important caveat, the implication of which should be considered here. Our V1 RF centres were within 7 deg of the centre of the fovea. In macaques, macular pigmentation is maximal at the fovea, but declines rapidly to negligible values by 8 deg eccentricity (Snodderly *et al.* 1991). This means that our central-most RFs could be influenced by a variable degree of pre-receptor absorption by macular pigment. Although our S-cone-isolating stimulus has been calculated without correction for macular pigment, this potential source of artefact is unlikely to have affected our results. Firstly, cells responding reliably to S-cone-isolating stimuli and cells that did not respond to S-cone-isolating stimuli were often encountered in the same track, were strongly driven through the same eye and their RFs largely overlapped (e.g. the two cells whose responses are illustrated in Fig. 1*A* and *B*). Secondly, as evident in the contrast response functions of the MT cell whose responses are shown in Fig. 1*C*, the magnitude of responses (average firing rate over one entire cycle of the stimulus) obtained for high-contrast S-cone-isolating stimuli was reached only with high-luminance contrasts. The contrast tuning curves reported here also follow the trend that has been reported previously on the basis of responses of a population of macaque area MT cells (see Fig. 4 of Seidemann *et al.* 1999 showing normalised population responses of S-cone input cells).

In the present study, in order to quantify the amount of S-cone input relative to the luminance-modulated input, an S-cone sensitivity index was calculated. The S-cone index for cells with a significant S-cone input varied between 0.3 and 1.6 (mean = 0.7, $n = 41$). For those cells, which did not show a significant response to S-cone-isolating stimuli, the S-cone indices ranged from 0 to 0.17 (mean = 0.05, $n = 45$). This relationship is shown in Fig. 1*D*, which is a plot of the peak firing rate calculated over 20 ms bins with no smoothing. While many cells that showed significant responses to S-cone modulation (open circles) also showed a response to luminance modulation, not all cells that showed a good response to luminance modulation exhibited a response to S-cone modulation. This result further supports our earlier conclusion that responses to S-cone modulation in our data are not attributable to luminance artefacts.

Because our sample contained a higher percentage of MT cells with robust S-cone inputs than the samples of MT cells examined in several previous studies (e.g. Seidemann *et al.* 1999; Barberini *et al.* 2005; Riecansky *et al.* 2005), we briefly sought to find out what this could be attributed to. One possibility is our use of flashing stationary stimuli instead of the moving stimuli traditionally used in studies of area MT. Figure 1*E* shows responses of one of the MT cells from our sample. Note that though this cell responds well to both diffuse flashed stimuli and drifting achromatic gratings (top panels), only the flashing S-cone-isolating stimuli evoke a vigorous response (see bottom panels). Similar results were obtained in six of the nine other cells that were tested. While we have not pursued this issue more systematically, we propose that moving stimuli activate inhibitory circuits that suppress the weaker S-cone signals either at the level of MT, or earlier in the visual pathway.

Reversible inactivation of V1

In order to study whether S-cone signals in area MT relay through area V1, we reversibly inactivated a part of V1 by cooling (25 cells) or by local iontophoresis of GABA (three cells). The eccentricities of the RF centres of MT cells subjected to this experiment ranged between 2 deg and 7 deg, matching the eccentricities of the classical RFs of cells in the part of area V1 that was inactivated. The size of the visual stimulus was restricted to be within the part of visual field representation in the V1 region that was directly under the Peltier device (see Methods, and later in Results for more details on this procedure). The majority (19/28) of the MT cells that showed reliable responses to S-cone-isolating stimuli showed significantly weaker responses to S-cone-isolating stimuli during inactivation of V1. Figure 2 shows the responses of an MT cell that

clearly exhibited this effect. The top panels show responses to luminance (left) and S-cone (right) modulation before cooling area V1. Note that responses to either stimulus were significantly reduced (Student's t tests, $P < 0.05$) during V1 cooling. The bottom panel shows recovery of the responses as early as 10 min after rewarming area V1 to 37°C. Although the response to luminance modulation was still apparent during cooling of V1, the response

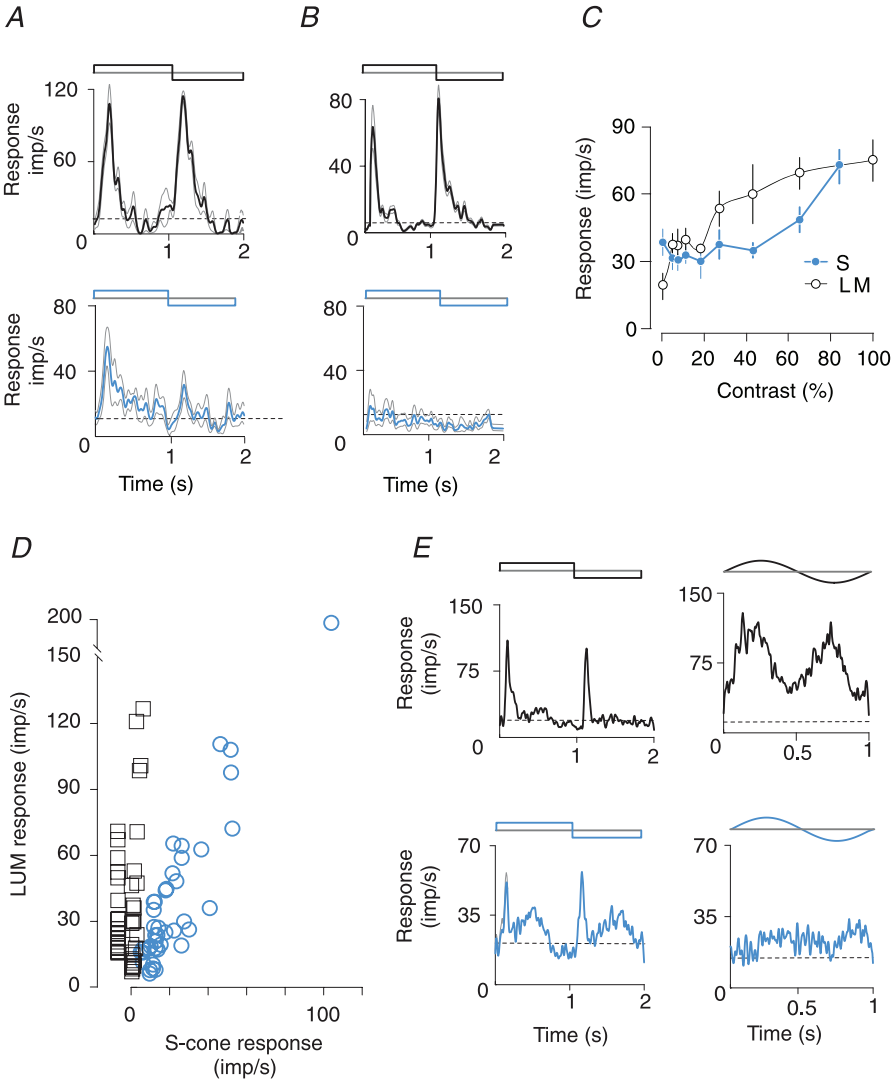

Figure 1. Responses of area MT neurons to achromatic and S-cone isolating visual stimuli
A and *B*, PSTHs of responses of an area MT cell receiving S-cone signals (*A*) and of another cell without detectable S-cone input (*B*). Upper PSTHs show responses to luminance contrast reversal, and lower PSTHs show responses to S-cone contrast reversal. The first half cycle of the stimulus was dark for luminance reversal and blue for S-cone contrast reversal. The length of each stimulus cycle was 2 s and binwidth was 20 ms. Both cells were recorded from the same electrode track and stimuli were presented through the same eye. *C*, amplitudes of the mean (0th harmonic) responses of the cell in *A* to stimuli of varying luminance and S-cone contrasts (TF = 4 Hz and SF = 1 cpd). Black lines are responses to stimuli varying in luminance. Blue lines are responses to stimuli that vary in S-cone contrast. Error bars represent the SEM. *D*, plot of the magnitude of responses of the MT neurones to luminance-modulated stimuli *vs.* the responses to S-cone-isolating stimuli. The squares indicate the magnitude of responses of MT units that did not show significant S-cone input, while the circles indicate the magnitude of responses of those MT units that responded to S-cone-isolating stimuli. *E*, left: PSTHs of responses of an area MT cell to flashing, contrast-reversing luminance-modulated (top) and S-cone-isolating (bottom) stimuli; right: PSTHs of responses of the same cell to moving luminance-modulating (top) and S-cone-isolating (bottom) grating stimuli (SF = 0.1 cpd). Note that unlike the response to luminance-modulated moving gratings, the response to the moving S-cone-isolating gratings is much weaker than that to flashing stationary S-cone-isolating stimuli. Dotted horizontal lines in all PSTHs (*A*, *B* and *E*) here and in Figs 2 and 3 indicate spontaneous firing rate during presentation of a uniform grey field of equal luminance.

to S-cone modulation completely disappeared during cooling of V1 (middle panel).

Figure 3 shows the variety of effects of V1 inactivation on MT cells. For each of the five cells illustrated there, responses to luminance-modulated (left columns) and S-cone-isolating (right columns) stimuli are shown before and during the inactivation. Responses of cells 1–4 were collected during inactivation of area V1 by cooling using the Peltier device, while in the case of cell 5, the inactivation was achieved by iontophoresis of GABA into V1. Note that cells 1, 2 and 5 exhibited significant reduction of responses during V1 inactivation (Student's t tests, $P < 0.05$), whereas responses of the other two MT cells (3 and 4) were not affected by the inactivation. Cells 1, 2 and 5 exhibited almost complete loss of responses to S-cone modulation during inactivation of V1. On the other hand, for luminance-modulated stimuli, cells 1 and 5 showed a near complete loss of response during V1 inactivation, but cell 2 showed only a reduction in the magnitude of response.

Figure 4 shows the data for all 28 MT cells with S-cone inputs in which responses were recorded before and during V1 inactivation. The figure plots, for each cell, the change in the magnitude of response to S-cone and luminance modulations brought about by the inactivation. Twelve out of the 28 cells showed a significant change in the magnitude of responses to both S-cone and luminance modulations (open circles), and in all but one of these cells the change was a decrease in the magnitude of responses. In seven other cells, there was a significant reduction for S-cone modulation, but not for luminance modulation (filled circles). The average magnitude of response for the 19 cells that showed a significant reduction in response to S-cone modulation during V1 inactivation was 47% of the control response. The average magnitude of response for the 12 cells that showed a significant reduction in response to luminance modulation during V1 inactivation was 41% of the control response. In seven cells, the inactivation had no significant effect on either S-cone or luminance modulation (filled squares). In two other cells, there was no significant change during cooling for S-cone modulation, but a change was observed for luminance modulation (open squares).

Our interpretation of the above results is that cells that showed no significant effect from the V1 inactivation received alternative inputs that bypassed area V1. However, one could argue that the lack of effect in some MT cells during striate cortical cooling may be due to inadequate cooling, especially when the striate representations of the visual stimuli might have been away from the centre of the cortical tissue directly under the Peltier probe. To address this issue, we have plotted in Fig. 5*A* and *C* the RF locations of the area MT cells with S-cone inputs – both those that showed a change during V1 cooling (Fig. 5*A*) and those that did not (Fig. 5*C*) – in relation to the visual field representation of the V1 cortex under the Peltier device ('Peltier field'). Furthermore, in Fig. 5*B* and *D* the locations and sizes of the visual stimuli used to activate these area MT cells are plotted in relation to the Peltier field. The shaded areas in these panels of Fig. 5 show the putative visual field representation on the cortex underneath the Peltier probe ('Peltier field'). This was reconstructed from recordings made near the corners of the Peltier probe in one animal. The RFs of MT neurones and the stimulus locations for this one animal are shown separately in Fig. 5*E* and *F*. The Peltier field shown includes the scatter and average extent of the V1 RFs (Dow *et al.* 1981), and not just their centres. Thus, we estimated the Peltier field to cover a trapezium in visual field with approximate dimensions of $6 \times 6.1 \times 6.3 \times 4$ deg. Admittedly, these dimensions are subject to some error due to the difficulty in accurate estimation of the location of the centre of fovea and the extrapolation of the 'Peltier field' from V1 recordings around the Peltier probe in one animal to the other three. However, we believe that this is not a serious cause for concern as, as we show below, the effective inactivation region is likely to be larger than the Peltier field.

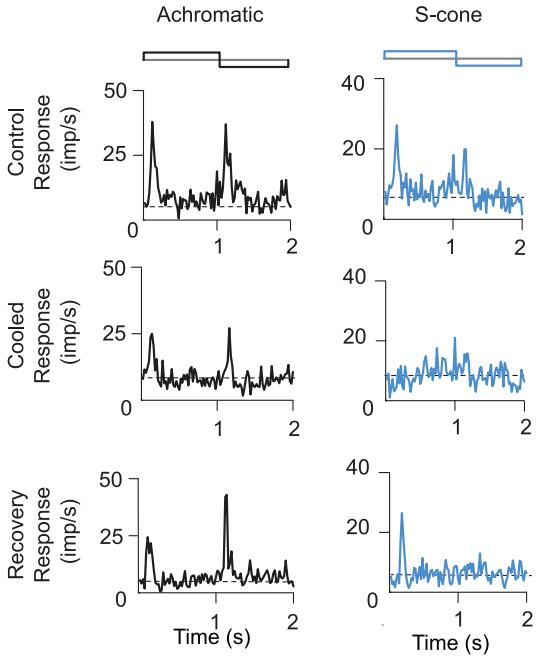

Figure 2. Effect of V1 inactivation on responses of an MT cell with S-cone input
The top panels show the PSTHs of control responses of this cell to luminance-modulated (left) and S-cone-isolating (right) stimuli. The middle panels show the PSTHs of responses of this cell during cooling of V1, and the bottom panels shows the recovery of the responses 10 min after rewarming of V1 to physiological temperatures. Stimulus parameters are the same as for cells whose responses are shown in Fig. 1*A* and *B*. To improve clarity of illustration, SEMs are not shown here or in Fig. 3. The SEMs shown in Fig. 1 are typical for our sample.

It can be seen from Fig. 5*B* and *D* that most, though not all, of the stimuli fall well within the Peltier field in V1. Figure 5 distinguishes between cells that showed significantly decreased responses to S-cone-modulating stimuli during V1 inactivation (black outlines in Fig. 5*A* and *B*) and those that did not (red outlines in Fig. 5*C* and *D*). There is no apparent difference between the distribution of the visual stimuli in Fig. 5*B* and *D* (but

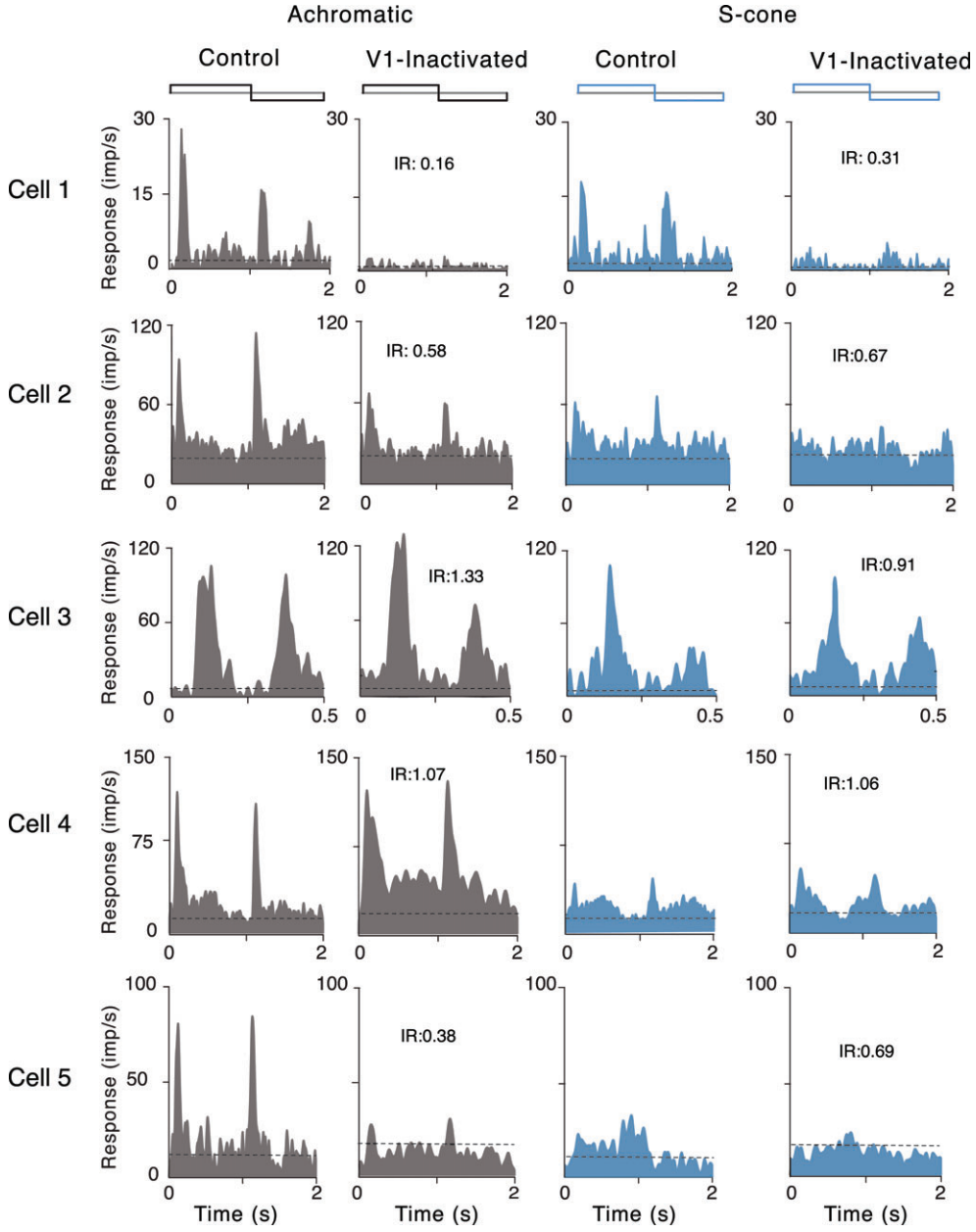

Figure 3. PSTHs of responses of area MT cells during inactivation of area V1 by cooling (cells 1–4) or inactivation by local iontophoretic injections of GABA (cell 5)
The two PSTHs on the left in each row show the responses to luminance modulation, and the two on the right the responses to S-cone modulation (first half of the stimulus cycle was dark and blue, respectively). The first and third columns show the responses in the control condition, and the second and fourth the responses during inactivation of V1. Note that cells 1 and 2 showed significant reduction in the magnitude of responses to S-cone-isolating stimulus during cooling of V1. The other two cells (3 and 4) did not show any reduction in the magnitude of responses during cooling of V1. Cell 5 shows significant changes in the magnitude of responses to S-cone-isolating and luminance-modulating stimuli during GABA inactivation of V1. Binwidth was 20 ms for all cells, except cell 3, for which it was 10 ms. IR represents inactivation ratio, i.e. ratio of the magnitude of response during inactivation to the magnitude of the control response as measured for the bin with peak activity (without removal of spontaneous firing rate).

also see later). To address further the question whether the inactivation seen in MT cell responses could be less as one presents the visual stimulus further out from the centre of the cortical surface under the Peltier device, we have plotted in Fig. 6 the degree of response change in the MT cell against the distance of the representation of the centre of the visual stimulus on the V1 surface from the centre of the inactivated region, which was calculated using the published cortical magnification factors (Dow *et al.* 1981) and our control V1 recordings. The figure shows no positive correlation either for S-cone modulation (Fig. 6*A*; Pearson coefficient, $r = 0.001$; $P > 0.99$) or for luminance modulation (Fig. 6*B*; Pearson coefficient, $r = -0.14$; $P > 0.5$). We are thus confident that any inadequate cooling due to the distance from the centre of the inactivated region was not a confounding factor in our results. In fact, we believe that the inactivation extended for many millimetres beyond the borders of the Peltier, as we have cooled the tissue directly under the Peltier probe down to about 3 deg, and this is likely to have cooled a considerable part of the surrounding cortex as well. The consequence of this can also be seen from the effective inactivation of the V1 input with many MT cells when using stimuli that fell partly outside the Peltier field – in fact this region seems to extend more for the affected cells than the unaffected (i.e. some of the black outlines in Fig. 6*B* extend past the red outlines in Fig. 6*D*).

Finally, we calculated the latencies of the responses to our contrast-reversing, luminance-modulated and S-cone-isolating stimuli. Although there was a difference in the mean latencies of responses of cells in which the S-cone signal seemed to bypass V1 and those of cells in which the S-cone signal did not bypass V1 (105.0 ± 23.1 ms, $n = 9$ *vs.* 116.29 ± 28.4 ms, $n = 19$, respectively), there is substantial variance and the difference does not reach statistical significance ($F = 0.865$, $P = 0.362$, ANOVA). The latencies of responses to luminance modulation also did not differ significantly between the control and V1 inactivated groups (84.7 ± 9.1 ms *vs.* 88.5 ± 20.2 ms, respectively, $F = 0.219$, $P = 0.645$, ANOVA). It is important to note in this context that in both groups, the latencies of responses to luminance modulation were significantly shorter than the latencies of responses to S-cone stimulation (ANOVA, $F = 4.659$, $P = 0.05$ for cells in which S-cone signals seem to bypass V1; and $F = 10.84$, $P = 0.02$ for cells affected by cooling, in which S-cone signal is presumably relayed through V1).

Discussion

We find that many area MT cells receive an excitatory input arising from the S-cones. Indeed, nearly half of our sample of MT cells showed a response to S-cone-isolating stimuli. This result is in agreement with other studies claiming that macaque's MT neurones respond to S-cone signals (Seidemann *et al.* 1998; Barberini *et al.* 2005; Riecansky *et al.* 2005). On the other hand, the existence of an S-cone input to MT has been questioned (Gegenfurtner *et al.* 1994). The main reason for this controversy may be the traditional use of moving line or drifting grating stimuli to stimulate area MT cells rather than the flashing stimuli used in this study. It is possible that the S-cone signal can be more readily conveyed in temporal square-wave presentations, which contain higher temporal frequency components that are absent in sine-wave presentations. Furthermore, transient signals may be suppressed when large moving patterns are used. Indeed, area V1 neurones, especially those in supragranular layers, receive inhibitory inputs from within V1 (for review, see Angelucci & Bressloff, 2006). Geniculate koniocellular cells, many of which carry S-cone signals (Martin *et al.* 1997; Roy *et al.* 2009), project directly to the supragranular layers of striate cortex (Casagrande *et al.* 2007). By contrast, the magnocellular signals to area MT are relayed via layer 4B of area V1, bypassing supragranular layers (Livingstone & Hubel, 1984, 1988). This in turn makes the magnocellular signals less susceptible to inhibitory influences mediated by horizontal connections, which are potentially more prominent in supragranular layers than in layer 4B (Kritzer *et al.* 1992).

Many MT cells continue to respond to achromatic visual stimuli during irreversible (Rodman *et al.* 1989)

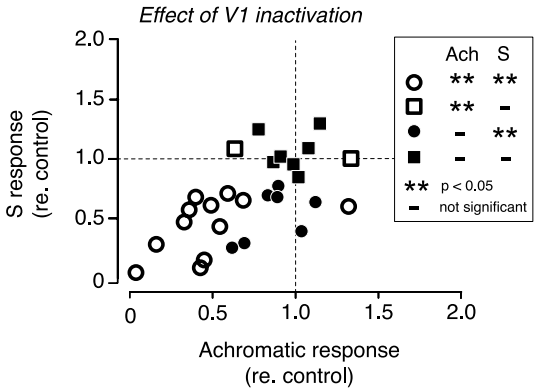

Figure 4. Responses of MT neurones with S-cone inputs to luminance-modulated stimuli *vs.* their responses to S-cone-isolating stimuli before and during inactivation of V1
The abscissa represents the ratio of the magnitude of achromatic response during V1 inactivation to the magnitude of control response. The ordinate represents the ratio of the magnitude of the response to S-cone modulation during V1 inactivation to the magnitude of control response. These measures are the same as the inactivation ratio, as defined in the legend to Fig. 3. The key on the right explains the symbols with reference to the significance (**) of the change in the magnitude of the response during V1 inactivation in the two stimulus conditions, viz. achromatic modulation (Ach) and S-cone modulation (S).

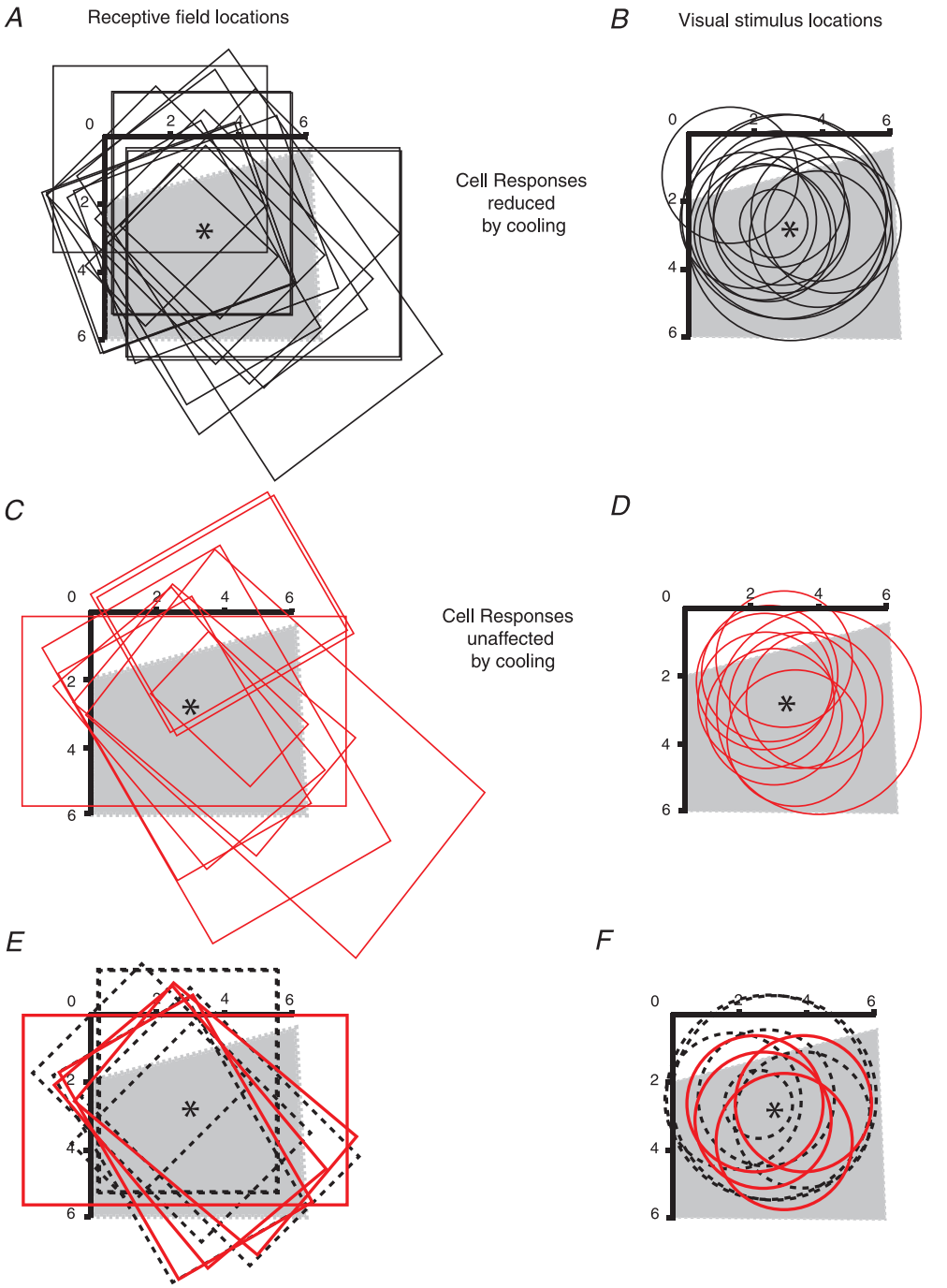

Figure 5. Relationship of MT receptive fields to the Peltier field on V1 and the visual stimuli used.
Visual field representations of striate cortex inactivated by cooling using the Peltier device (grey shaded area) and the RF outlines of area MT cells recorded during cooling (*A*, *C*), and the locations and sizes of the visual stimuli used to stimulate them (*B*, *D*). *A* and *B*, the black outlines pertain to cells that showed significant reduction of the response for S-cone modulation during cooling, while the red outlines in *C* and *D* pertain to those MT cells that did not show significant changes in response to S-cone modulation during cooling of striate cortex. *E* and *F*, the subset of cells from *A*–*D* that came from one animal where the extent of the 'Peltier field' (cortex directly beneath the Peltier probe) was ascertained by recordings. The dashed black outlines in *E* and *F* refer to cells whose responses were significantly reduced by cooling, while the solid red outlines refer to cells whose responses were unaffected by the cooling. The centre of the Peltier element (*) was at the part of V1 representing a visual field eccentricity of 3 deg. Note that in these panels this is away from the centre of the shaded area due to the higher cortical magnification factor of the representation of the centre of the fovea. The horizontal and vertical black scales with degrees marked from 0 to 6 refer to the representations of the horizontal and vertical meridians, respectively.

or reversible (Girard & Bullier, 1989) inactivation of ipsilateral area V1. Indeed, to abolish responses of macaque's MT neurones to achromatic stimuli, Rodman *et al.* (1990) had to inactivate both the ipsilateral V1 and the ipsilateral superior colliculus. Though V1 inactivation had little effect on a small proportion of MT cells (7/28) in our sample, the majority showed significant reductions. We found that responses to S-cone-isolating stimuli as well as responses to achromatic stimuli can be reduced during V1 inactivation. Overall, our results show that both luminance signals and S-cone signals arrive at single MT neurones, in some cases via area V1 and in others bypassing V1. Despite the classical view that koniocellular signals only project to V1 blobs and then on to area V4 via so-called thin cytochrome-oxidase stripes in V2 (Livingstone & Hubel, 1988; Zeki & Shipp, 1988), it is now known that there is considerable mixing of the three pathways (Sincich & Horton, 2005). Mixing may happen in area MT (Maunsell *et al.* 1990), in projections of V1 compartments to V2 (Sincich & Horton, 2005), and/or even earlier in area V1, as there is both anatomical (Yoshioka *et al.* 1994; Yabuta & Callaway, 1998; Casagrande *et al.* 2007) and physiological (Nealy & Maunsell, 1994; Vidyasagar *et al.* 2002) evidence that is consistent with early convergence of signals. More specifically, one possibility for convergence of magnocellular and koniocellular pathways in striate cortex are koniocellular axonal arbors in layer 1 contacting apical dendrites of layer 4B cells that project to area MT. Another possibility is via the axonal arbours of geniculate koniocellular afferents that often stray into interblob regions within area V1 (see Casagrande *et al.* 2007; Fig. 4). These interblob regions of V1 are known to project to the thick cytochrome-oxidase stripes in V2 that constitute the main V2 inputs to MT (Sincich & Horton, 2002).

Though during the cooling phases the thermistor in area V1 showed temperatures of 10°C at a depth of 1 mm, the persistence of responses to L-cone and M-cone modulation, but not S-cone modulation, can potentially

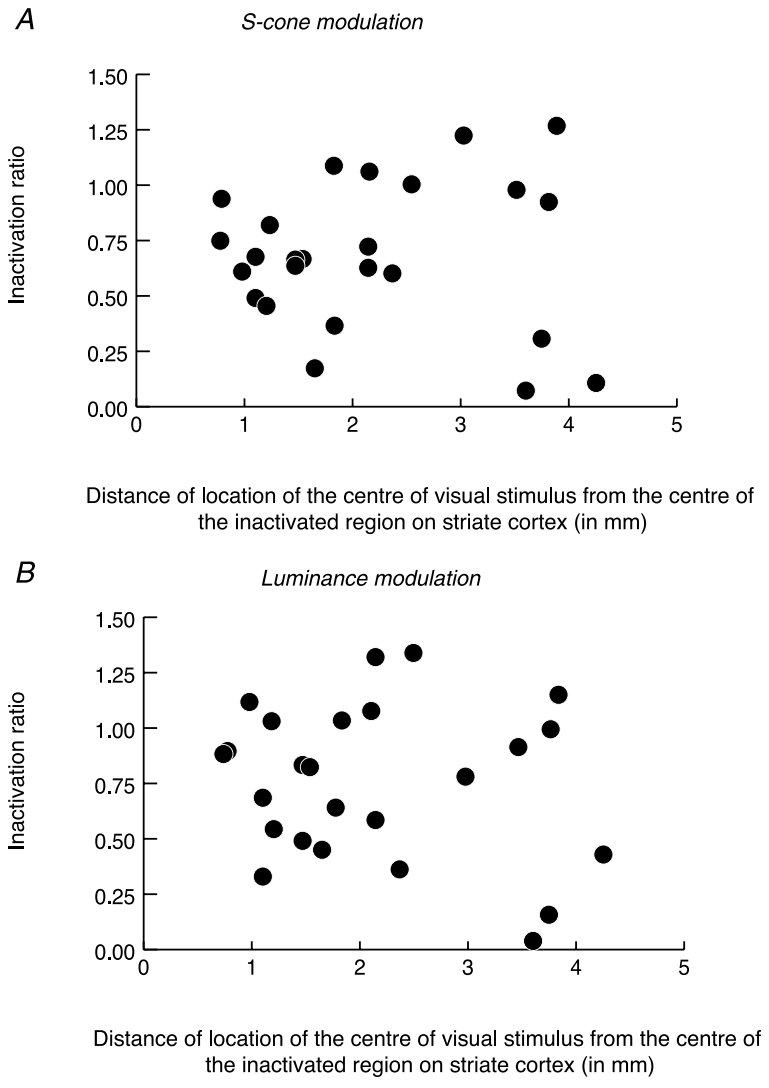

Figure 6. Relationship between inactivation ratio of area MT cells with S-cone inputs and distance of the representation of the visual stimulus from the centre of the cooled region on area V1
A and *B*, the relationship for S-cone modulation and for luminance modulation, respectively. Inactivation ratio is the ratio of the magnitude of the response during cooling to the magnitude of control response.

also be explained by alternative interpretations rather than by existence of inputs to MT that bypass V1. One such interpretation may be a stronger drive from L- and M-cones than from S-cones to the V1 cells that provide the input to the MT cell. On the other hand, it is also possible that the S-cone signal relays to V2 and on to MT via layer 3 cells and layer 1 afferents in V1, whereas the M- and L-cone inputs are carried by the magnocellular relay via layer 4B cells (e.g. Zeki, 1978; Livingstone & Hubel, 1984, 1988; Gegenfurtner, 2003). Layer 4B cells, being at a greater depth, may be less affected by cooling than layer 3 cells. This is, however, less likely. Our controls (see Methods) show that maintaining a temperature of 2.8°C at the dura would effectively reduce temperatures in layer 4 to 10°C, a low enough temperature when all spike activity is suppressed (Volgushev *et al.* 2000). Furthermore, because even at temperatures as high as 15–20°C, synaptic transmission is very seriously slowed down (Volgushev *et al.* 2000), one should see latency changes in the response to M- and L-cone signals relayed via V1. However, no such latency increase is evident in our data (as, for example, in the responses of cell 2 in Fig. 3, second column).

The source of the alternative input to MT that bypasses V1 could be pulvinar and/or the LGN (Sincich *et al.* 2004; Kaas & Lyon, 2007). Pulvinar is known to have strong reciprocal connections with MT (Kaas & Lyon, 2007), and it has been shown recently in the macaque that the collicular input to MT need not involve a polysynaptic route within the pulvinar. Indeed, relay neurones within macaque's inferior pulvinar receive direct inputs from the superior colliculus and project directly to MT (Berman & Wurtz, 2010). Pulvinar is also known to receive direct, albeit sparse, projection from the retina (Mizuno *et al.* 1982; Itaya & Van Hoesen, 1983; Nakagawa & Tanaka, 1984; Cowey *et al.* 1994; O'Brien *et al.* 2001; Warner *et al.* 2010). An alternative, but not mutually exclusive, possibility is that the direct projection from koniocellular layers of LGN to MT (Sincich *et al.* 2004) includes cells with strong S-cone inputs (Martin *et al.* 1997; Roy *et al.* 2009). The main source of the S-cone signals to MT that bypass V1 is less likely to be the superior colliculus, as there appears to be little chromatically opponent input to the superior colliculus (Marrocco & Li, 1977; Schiller & Malpeli, 1977; Martin *et al.* 2012). Moreover, in humans with blindsight, the collicular pathway mediating MT activation does not involve S-cone signals (Leh *et al.* 2009). A recent study in the macaque showed that after inactivation of the LGN, there is little activity in extra-striate cortical areas, thus casting further doubt on the efficacy of the colliculo-pulvinar route (Schmid *et al.* 2010). This also raises the possibility that inputs to MT from different sources are too weak to produce responses when activated in isolation, but they may be effective when acting in combination.

Our results on the latencies of spike responses of MT cells to visual stimulation show that the achromatic input is significantly faster than the input carrying S-cone signals in both the route relaying via V1 and that bypassing V1. On the other hand, comparison of the latencies of responses of MT neurones between the two routes does not unequivocally support the idea (ffytche *et al.* 1995) that the direct pathway to MT that bypasses V1 is faster. In particular, although our data do reveal a tendency in this direction, the latency differences are not statistically significant.

What could possibly be the function of the S-cone pathway to the dorsal stream, which has also been reported in human MT+/V5 (Morand *et al.* 2000)? We believe that as an evolutionarily older pathway (Nathans, 1999; Casagrande & Xu, 2004; Johnson *et al.* 2010), an S-cone pathway might essentially be a complementary channel to the luminance pathway and may under some circumstances substitute for it.

Conclusions

The present study provides physiological evidence of S-cone signals reaching a dorsal stream cortical region, area MT through at least two pathways – one relaying via area V1 and the other as a direct projection from the koniocellular regions of the LGN and/or from the pulvinar, thus bypassing area V1.

References

Albright TD (1984). Direction and orientation selectivity of neurons in the visual area MT of the macaque. *J Neurophysiol* **52**, 1106–1130.

Angelucci A & Bressloff PC (2006). Contribution of feedforward, lateral and feedback connections to the classical receptive field center and extra-classical receptive field surround of primate V1 neurons. *Prog Brain Res* **154**, 93–120.

Barberini CL, Cohen MR, Wandell BA & Newsome WT (2005). Cone signal interactions in direction-selective neurons in the middle temporal visual area (MT). *J Vision* **5**, 603–621.

Barlow HB, Blakemore C & Pettigrew JD (1967). The neural mechanism of binocular depth discrimination. *J Physiol* **193**, 327–342.

Berman RA & Wurtz RH (2010). Functional identification of a pulvinar path from superior colliculus to cortical area MT. *J Neurosci* **30**, 6342–6354.

Casagrande VA & Xu X (2004). Parallel visual pathways: a comparative perspective. In *The Visual Neurosciences*, ed. Chalupa LM and Werner JS, pp. 494–506. MIT Press Cambridge, USA.

Casagrande VA, Yazar F, Jones KD & Ding Y (2007). The morphology of the koniocellular axon pathway in the macaque monkey. *Cereb Cortex* **17**, 2334–2345.

Cowey A (2004). The 30th Sir Frederick Bartlett Lecture: fact, artefact, and myth about blindsight. *QJ Exp Psychol A* **57**, 577–609.

Cowey A, Stoerig P & Bannister M (1994). Retinal ganglion cells labelled from the pulvinars nucleus in macaque monkeys. *Neuroscience* **61**, 691–705.

DeYoe EA & Van Essen DC (1988). Concurrent processing streams in monkey visual cortex. *Trends Neurosci* **11**, 219–226.

Dobkins KR & Albright TD (1994). What happens if it changes color when it moves?: the nature of chromatic input to macaque visual area MT. *J Neurosci* **14**, 4854–4870.

Dow BM, Snyder AZ, Vautin RG & Bauer R (1981). Magnification factor and receptive field size in foveal striate cortex of the monkey. *Exp Brain Res* **44**, 213–228.

ffytche DH, Guy CN & Zeki S (1995). The parallel visual motion inputs into areas V1 and V5 of human cerebral cortex. *Brain* **118**, 1375–1394.

Gattass R, Gross CG & Sandell JH (1981). Visual topography of V2 in the macaque. *J Comp Neurol* **201**, 519–539.

Gegenfurtner KR (2003). Cortical mechanisms of color vision. *Nature Rev Neurosci* **4**, 563–572.

Gegenfurtner KR & Hawken MJ (1996). Interaction of motion and color in the visual pathways. *Trends Neurosci* **19**, 394–401.

Gegenfurtner KR, Kiper DC, Beusmans JM, Carandini M, Zaidi Q & Movshon JA (1994). Chromatic properties of neurons in macaque MT. *Vis Neurosci* **11**, 455–466.

Girard P & Bullier J (1989). Visual activity in area V2 during reversible inactivation of area 17 in the macaque monkey. *J Neurophysiol* **62**, 1287–1302.

Girard P, Salin PA & Bullier J (1992). Response selectivity of neurons in area MT of the macaque monkey during reversible inactivation of area V1. *J Neurophysiol* **67**, 1437–1446.

Hupé JM, Chouvet G & Bullier J (1999). Spatial and temporal parameters of cortical inactivation by GABA. *J Neurosci Methods* **86**, 129–143.

Itaya SK & Van Hoesen GW (1983). Retinal projections to the inferior and medial pulvinar nuclei in the old-world monkey. *Brain Res* **269**, 223–230.

Jayakumar J, Roy S, Dreher B & Vidyasagar TR. (2009). S-cone signals to area MT in the macaque: some bypass area V1 and others do not. *Soc Neurosci. Abst., Annual Meeting*, *Chicago.*

Johnson EN, Van Hooser SD & Fitzpatrick D (2010). The representation of S-cone signals in primary visual cortex. *J Neurosci* **30**, 10337–10350.

Kaas JH & Lyon DC (2007). Pulvinar contributions to the dorsal and ventral streams of visual processing in primates. *Brain Res Rev* **55**, 285–296.

Komatsu H & Wurtz RH (1988). Relation of cortical areas MT and MST to pursuit eye movements. I. Localization and visual properties of neurons. *J Neurophysiol* **60**, 580–603.

Kritzer MF, Cowey A & Somogyi P (1992). Patterns of inter- and intralaminar GABAergic connections distinguish striate (V1) and extrastriate (V2, V4) visual cortices and their functionally specialized subdivisions in the Rhesus monkey. *J Neurosci* **12**, 4545–4564.

Lagae L, Maes H, Raiguel S, Xiao D-K & Orban GA (1994). Responses of macaque STS neurons to optic flow components: a comparison of areas MT and MST. *J Neurophysiol* **71**, 1597–1626.

Lamb TD (1995). Photoreceptor spectral sensitivities: common shape in the long-wavelength region. *Vision Res* **35**, 3083–3091.

Leh SE, Ptito A, Schönwiesner M, Chakravarty MM & Mullen KT (2009). Blindsight mediated by an S-cone-independent collicular pathway: an fMRI study in hemispherectomized subjects. *J Cogn Neurosci* **22**, 670–682.

Livingstone MS & Hubel DH (1984). Anatomy and physiology of a color system in the primate visual cortex. *J Neurosci* **4**, 309–356.

Livingstone MS & Hubel DH (1988). Seregation of form, color, movement and depth: anatomy, physiology and perception. *Science* **240**, 74–749.

Marrocco RT & Li RH (1977). Monkey superior colliculus: properties of single cells and their afferent inputs. *J Neurophysiol* **40**, 844–860.

Martin PR, Tailby C, Solomon SG, Cheong S-K & Pietersen ANJ (2012). Contribution of short wavelength sensitive (S or "blue" cones) to visual responses in superior colliculus. *Proc Aust Neurosci Soc* 130.

Martin PR, White AJ, Goodchild AK, Wilder HD & Sefton AE (1997). Evidence that blue-on cells are part of the third geniculocortical pathway in primates. *Eur J Neurosci* **9**, 1536–1541.

Maunsell JH & Gibson JR (1992). Visual response latencies in striate cortex of the macaque monkey. *J Neurophysiol* **68**, 1332–1344.

Maunsell JH, Nealey TA & DePriest DD (1990). Magnocellular and parvocellular contributions to responses in the middle temporal visual area (MT) of the macaque monkey. *J Neurosci* **10**, 3323–3334.

Maunsell JH & van Essen DC (1983). The connections of the middle temporal visual area (MT) and their relationship to a cortical hierarchy in the macaque monkey. *J Neurosci* **3**, 2563–2586.

Mizuno N, Itoh K, Uchida K, Uemura-Sumi M & Matsushita R (1982). A retino-pulvinar projection in the macaque monkey as visualized by the use of anterograde transport of horseradish peroxidase. *Neurosci Lett* **30**, 199–203.

Morand S, Thut G, de Peralta RG, Clarke S, Khateb A, Landis T & Michel CM (2000). Electrophysiological evidence for fast visual processing through the human koniocellular pathway when stimuli move. *Cereb Cortex* **10**, 817–825.

Nakagawa S & Tanaka S (1984). Retinal projections to the pulvinar nucleus of the macaque monkey: a re-investigation using autoradiography. *Exp Brain Res* **57**, 151–157.

Nassi JJ, Lyon DC & Callaway EM (2006). The parvocellular LGN provides a robust disynaptic input to the visual motion area MT. *Neuron* **50**, 319–327.

Nathans J (1999). The evolution and physiology of human color vision: insights from molecular genetic studies of visual pigments. *Neuron* **24**, 299–312.

Nealy TA & Maunsell JH (1994). Magnocellular and parvocellular contributions to the responses of neurons in macaque striate cortex. *J. Neurosci* **14**, 2069–2079.

O'Brien BJ, Abel PL & Olavarria JF (2001). The retinal input to calbindin-D28k-defined subdivisions in macaque inferior pulvinar. *Neurosci Lett* **312**, 145–148.
Riecansky I, Thiele A, Distler C & Hoffmann KP (2005). Chromatic sensitivity of neurones in area MT of the anaesthetised macaque monkey compared to human motion perception. *Exp Brain Res* **167**, 504–525.
Rodman HR, Gross CG & Albright TD (1989). Afferent basis of visual response properties in area MT of the macaque. I. Effects of striate cortex removal. *J Neurosci* **9**, 2033–2050.
Rodman HR, Gross CG & Albright TD (1990). Afferent basis of visual response properties in area MT of the macaque. II. Effects of superior colliculus removal. *J Neurosci* **10**, 1154–1164.
Roy S, Jayakumar J, Martin PR, Dreher B, Saalmann YB, Hu D & Vidyasagar TR (2009). Segregation of short-wavelength-sensitive (S) cone signals in the macaque dorsal lateral geniculate nucleus. *Eur J Neurosci* **30**, 1517–1526.
Saito H, Tanaka K, Isono H, Yasuda M & Mikami A (1989). Directionally selective response of cells in the middle temporal area (MT) of the macaque monkey to the movement of equiluminous opponent color stimuli. *Exp Brain Res* **75**, 1–14.
Schiller PH & Malpeli JG (1977). Properties and tectal projections of monkey retinal ganglion cells. *J Neurophysiol* **40**, 428–445.
Schmid MC, Mrowka SW, Turchi J, Saunders RC, Wilke M, Peters AJ, Ye FQ & Leopold DA (2010). Blindsight depends on the lateral geniculate nucleus. *Nature* **466**, 373–377.
Seidemann E, Poirson AB, Wandell BA & Newsome W (1999). Color signals in area MT of the macaque monkey. *Neuron* **24**, 911–917.
Sincich LC & Horton JC (2002). Divided by cytochrome oxidase: a map of the projections from V1 to V2 in macaques. *Science* **295**, 1734–1737.
Sincich LC & Horton JC (2005). The circuitry of V1 and V2: integration of color, form, and motion. *Annu Rev Neurosci* **28**, 303–326.
Sincich LC, Park KF, Wohlgemuth MJ & Horton JC (2004). Bypassing V1: a direct geniculate input to area MT. *Nat Neurosci* **7**, 1123–1128.
Snodderly DM, Handelman GJ & Adler AJ (1991). Distribution of individual macular pigment carotenoids in central retina of macaque and squirrel monkeys. *Invest Ophthalmol Vis Sci* **32**, 268–279.
Vakalopoulos C (2005). A theory of blindsight – the anatomy of the unconscious: a proposal for the koniocellular projections and intralaminar thalamus. *Med Hypotheses* **65**, 1183–1190.
Vidyasagar TR, Kulikowski JJ, Lipnicki DM & Dreher B (2002). Convergence of parvocellular and magnocellular information channels in the primary visual cortex of the macaque. *Eur J Neurosci* **16**, 945–956.
Volgushev M, Vidyasagar TR, Chistiakova M & Eysel UT (2000). Synaptic transmission in the neocortex during reversible cooling. *Neuroscience* **98**, 9–22.
Wandell BA, Poirson AB, Newsome WT, Baseler HA, Boynton GM, Huk A, Gandhi S & Sharpe LT (1999). Color signals in human motion-selective cortex. *Neuron* **24**, 901–909.
Warner CF, Goldschmit Y & Bourne JA (2010). Retinal afferents synapse with relay cells targeting the middle temporal area in the pulvinar and lateral geniculate nuclei. *Front Neuroanat* **4**, 8.
Weiskrantz L, Warrington EK, Sanders MD & Marshall J (1974). Visual capacity in the hemianopic field following a restricted occipital ablation. *Brain* **97**, 709–728.
Wyszecki G & Stiles WS (1982). *Color Science: Concepts and Methods, Quantitative Data and Formulae*. Wiley, New York.
Yabuta NH & Callaway EM (1998). Functional streams and local connections of layer 4C neurons in primary visual cortex of the macaque monkey. *J Neurosci* **18**, 9489–9499.
Yoshioka T, Levitt JB & Lund JS (1994). Independence and merger of thalamocortical channels within macaque monkey primary visual cortex: anatomy of interlaminar projections. *Vis Neurosci* **11**, 467–489.
Zeki S (1978). Functional specialisation in the visual cortex of the rhesus monkey. *Nature* **274**, 423–428.
Zeki S & Shipp (1988) The functional logic of cortical connections. *Nature* **335**, 311–317.

Author contributions

B.D., P.R.M. and T.R.V. conceptualized and designed the experiments; J.J., S.R., B.D., P.R.M. and T.R.V. performed the experiments; J.J., S.R. and T.R.V. analysed the data; J.J. and T.R.V. drafted the manuscript; J.J., B.D., P.R.M. and T.R.V. edited and revised the manuscript for critical intellectual content. All authors have approved the final version of the manuscript. Experiments were performed at the University of Melbourne.

Acknowledgements

We thank Ana Lara for technical assistance and Will Dobbie for computer programming. This study was supported by project grants 509254 and APP1004102 from the Australian National Health and Medical Research Council.